

Supplementary Information

for

Amyloid Fibril Formation of Human Recombinant Insulin Due to the Interfacial Hydrophobicity of Fluorocarbon Polymer Membranes

Kengo Mitsuya¹; Shingo Tsurumoto¹; Yuya Kurosawa¹; Ryotaro Koga¹; Takehisa Hanawa¹; and Satoru Goto^{1,2,*}

¹*Faculty of Pharmaceutical Sciences, Tokyo University of Science, 6-3-1, Niijuku, Katsushika, Tokyo, 125-8585 Japan, and* ²*Research Institute for Science and Technology, Tokyo University of Science, 6241 Yamazaki, Noda, Chiba, 278-8510 Japan.*

*To whom correspondence should be addressed: s.510@rs.tus.ac.jp

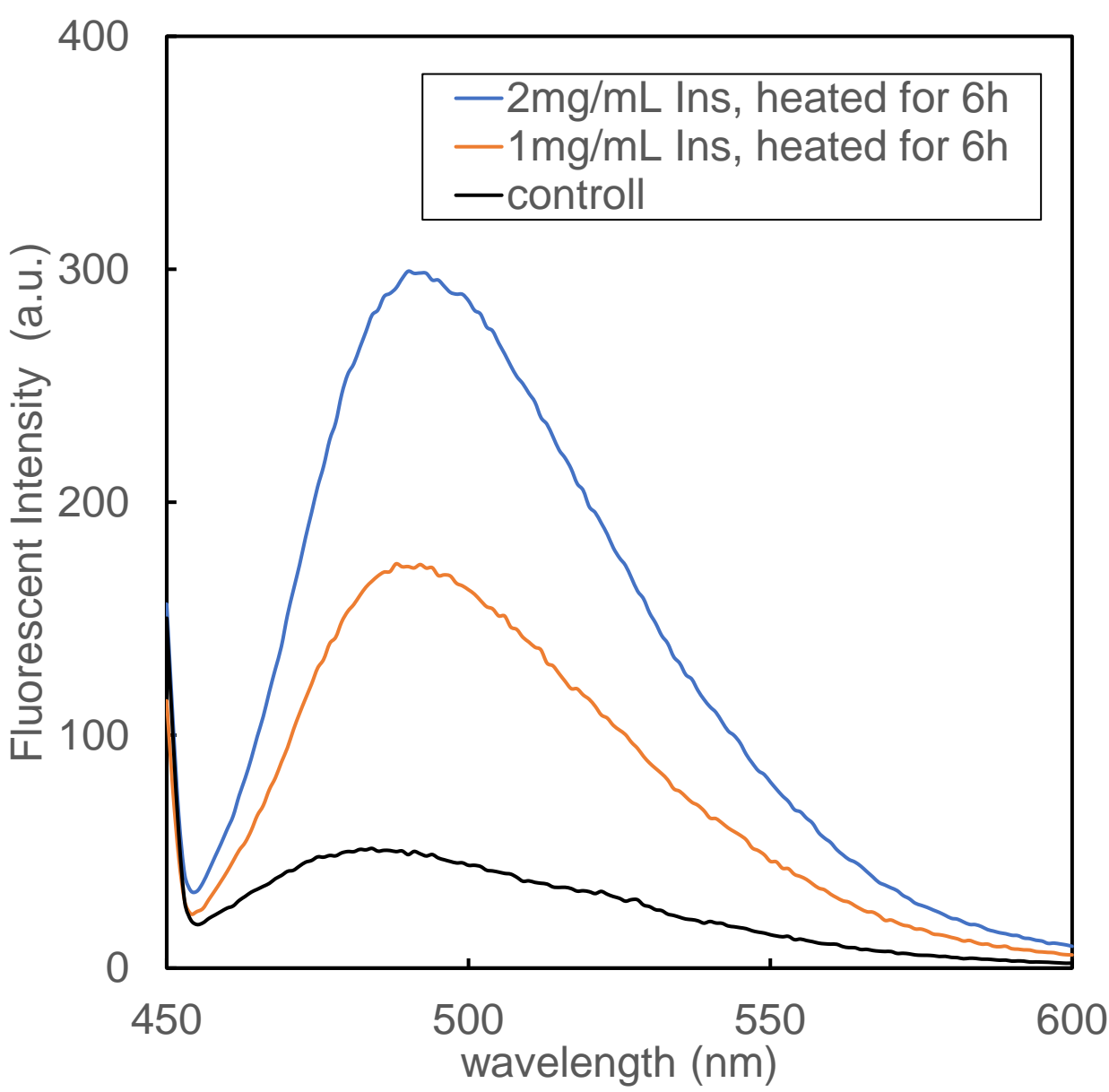


Figure S1. Thioflavin T (ThT) fluorescence spectra of 1 mg/mL (blue) and 2 mg/mL (amber) insulin (INS) in buffer solutions (pH 1.6), which were heated at 338 K (65°C) for 6 hr. The final ThT concentration is 50 μ M, and the control spectrum, obtained in the absence of INS, is shown in black. The peaks at 488 nm were observed.

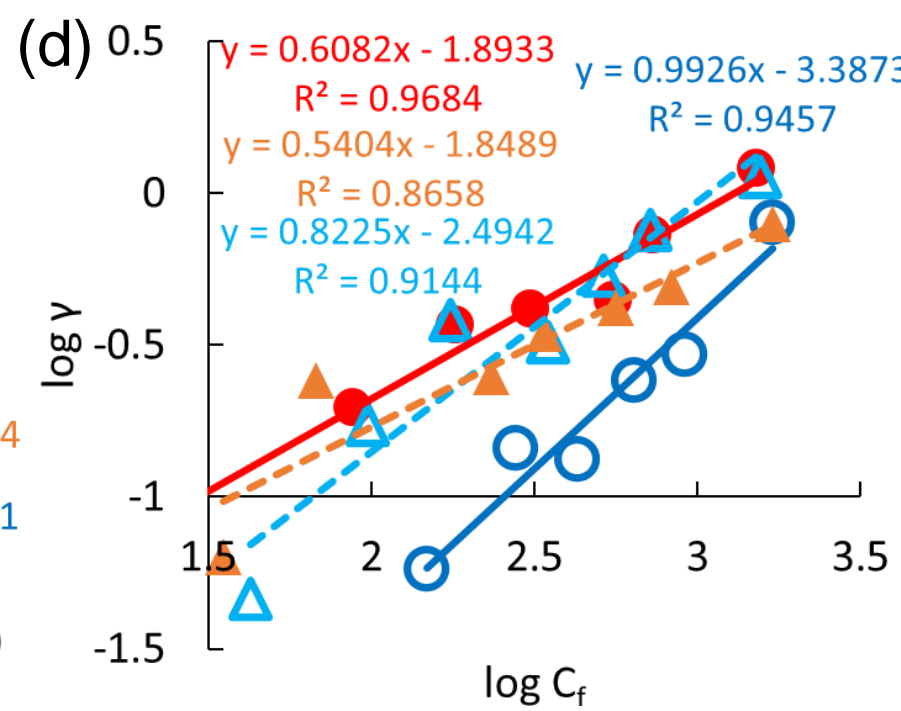
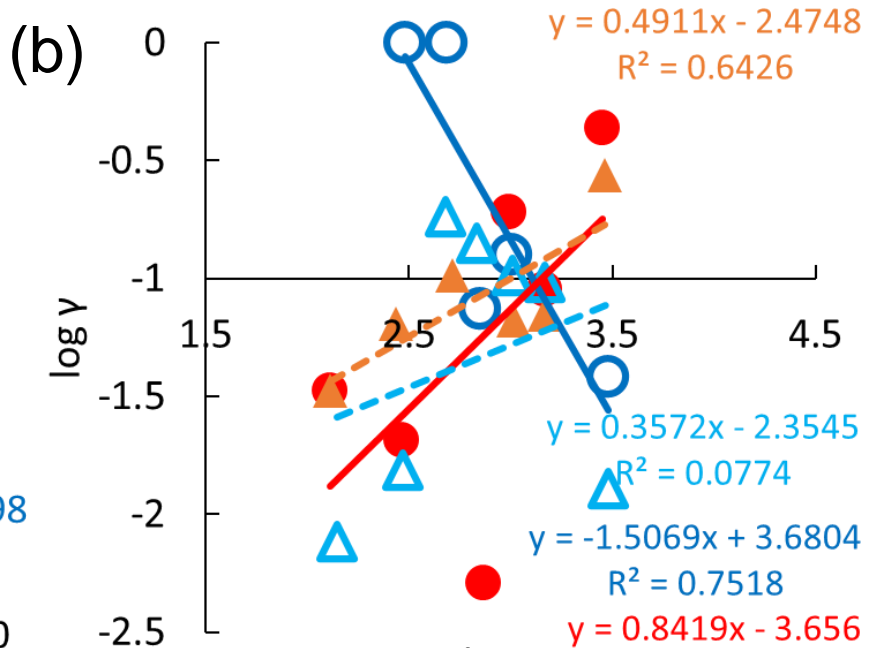
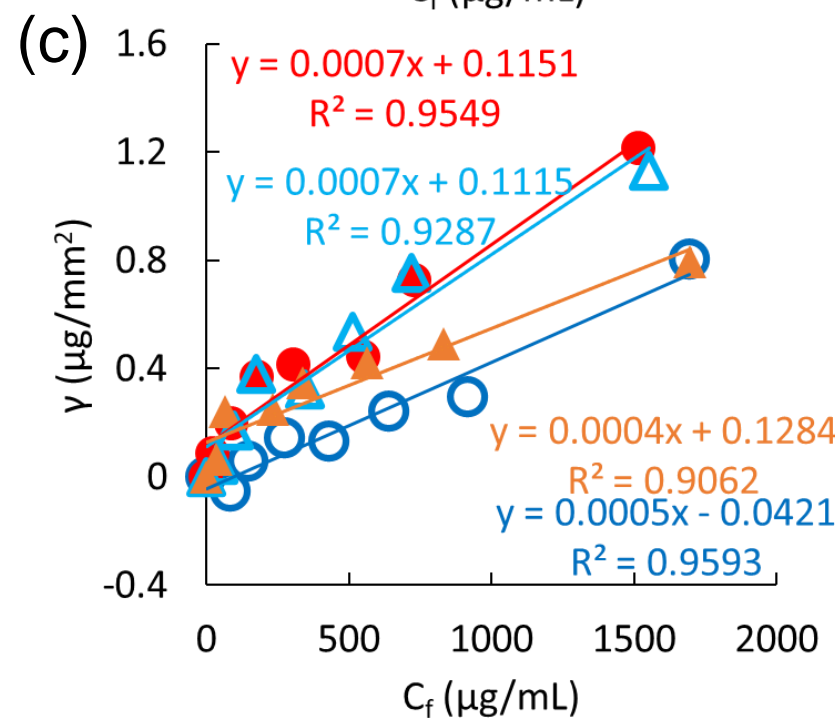
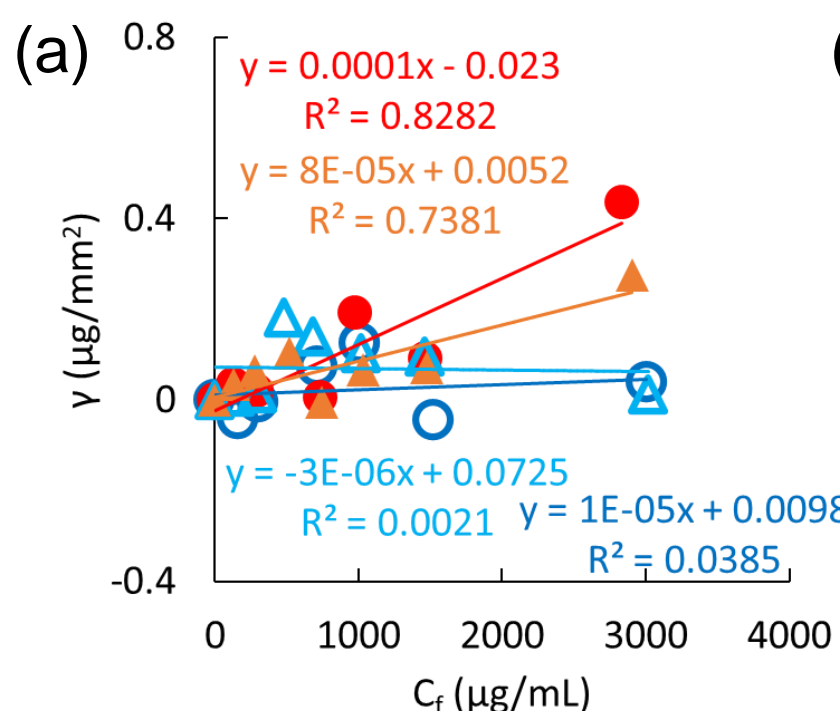


Figure S2. Analyses of BSA (a and b) and ConA (c and d) adsorption on the FCP membranes: hydrophilic (blue open circles) and hydrophobic PVDF (red closed circles), and hydrophilic (light blue open triangles) and hydrophobic PTFE (amber closed triangles), based on Henry's equation (a and c) and Freundlich's equation (b and d).

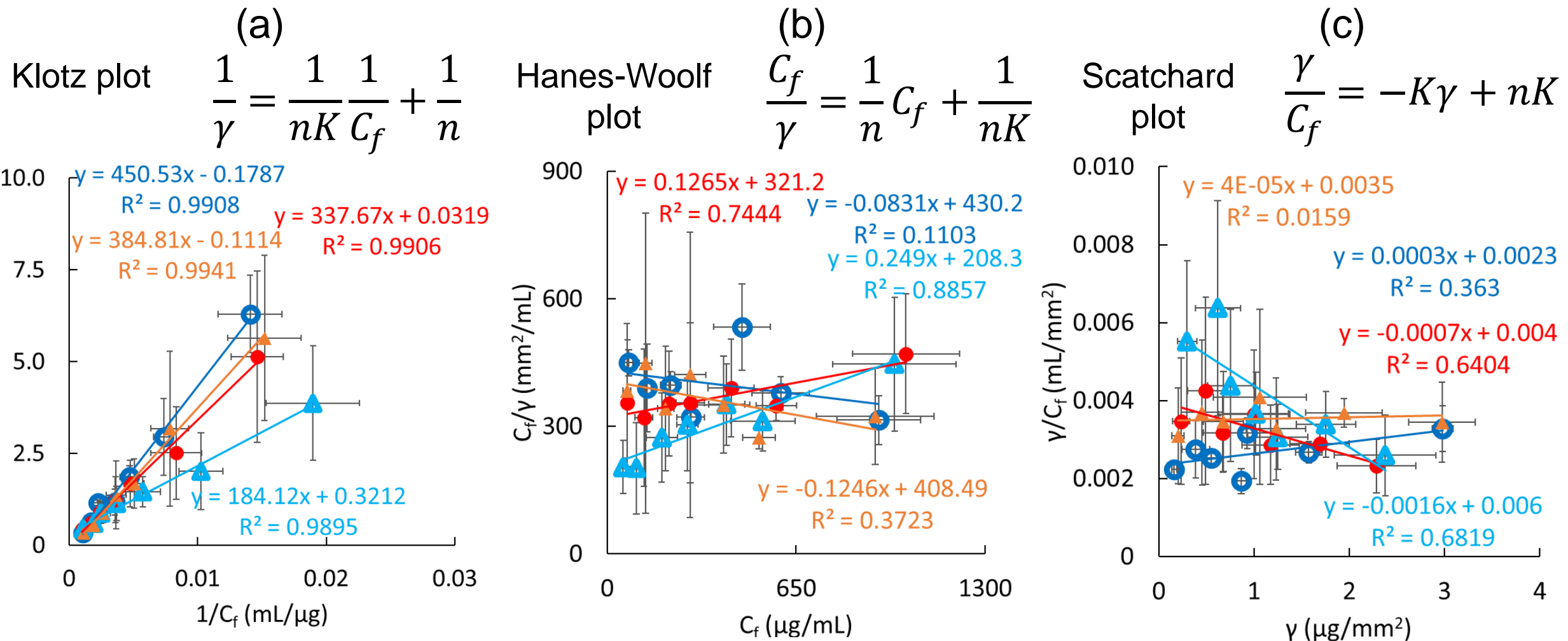


Figure S3. Analyses of heat-treated INS adsorptions on FCP membranes: hydrophilic (blue open circles) and hydrophobic PVDF (red closed circles), and hydrophilic (light blue open triangles) and hydrophobic PTFE (amber closed triangles), based on Klotz's (a), Hanes-Woolf's (b), and Scatchard's plots (c). Error bars on the ordinate and abscissa were expressent standard deviations from three or more experiments.

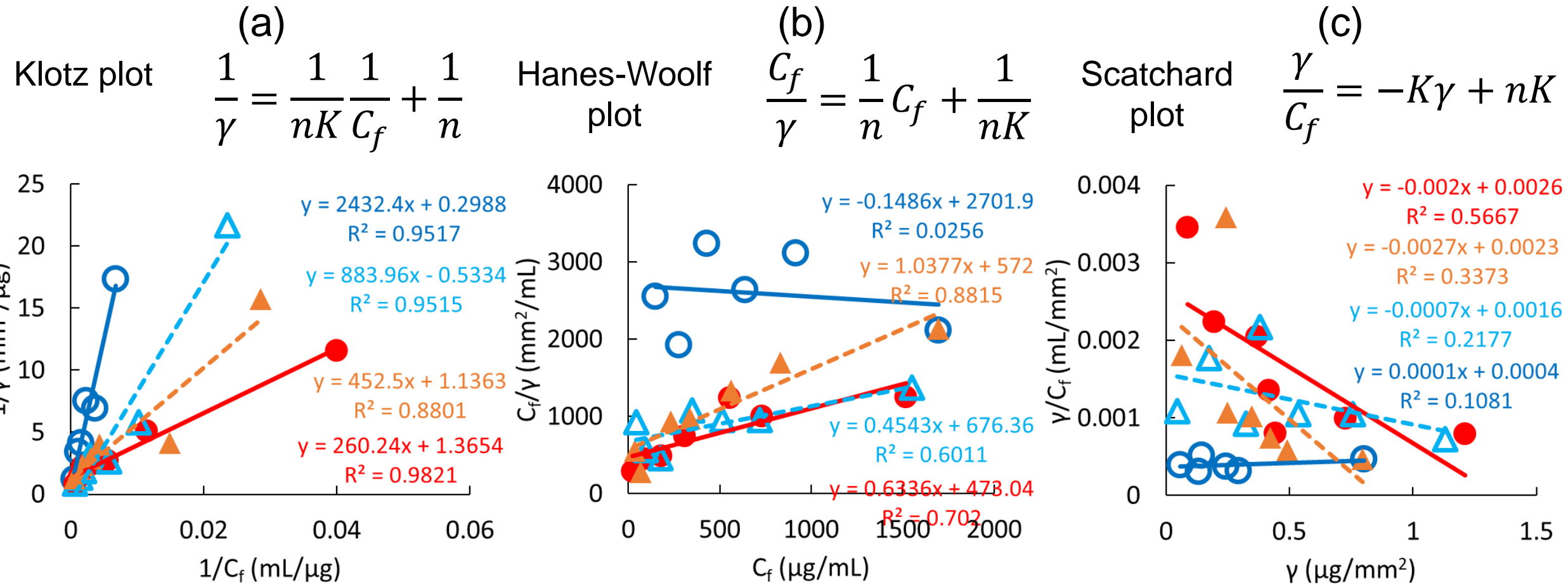


Figure S4. Analyses of ConA adsorptions on the FCP membranes: hydrophilic (blue open circles) and hydrophobic PVDF (red closed circles), as well as hydrophilic (light blue open triangles) and hydrophobic PTFE (amber closed triangles), based on Klotz's (a), Hanes-Woolf's (b), and Scatchard's plots (c).

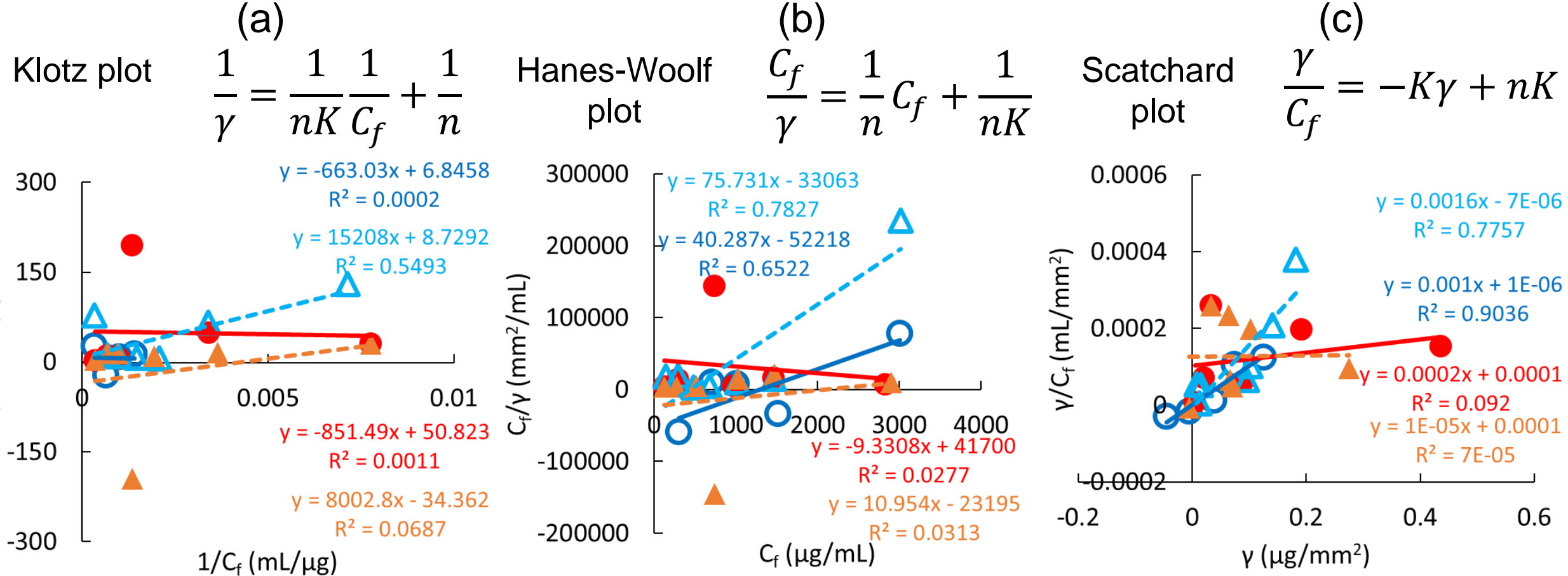


Figure S5. Analyses of BSA adsorption on FCP membranes: hydrophilic (blue open circles) and hydrophobic PVDF (red closed circles), as well as hydrophilic (light blue open triangles) and hydrophobic PTFE (amber closed triangles), based on Klotz's (a), Hanes-Woolf's (b), and Scatchard's plots (c).

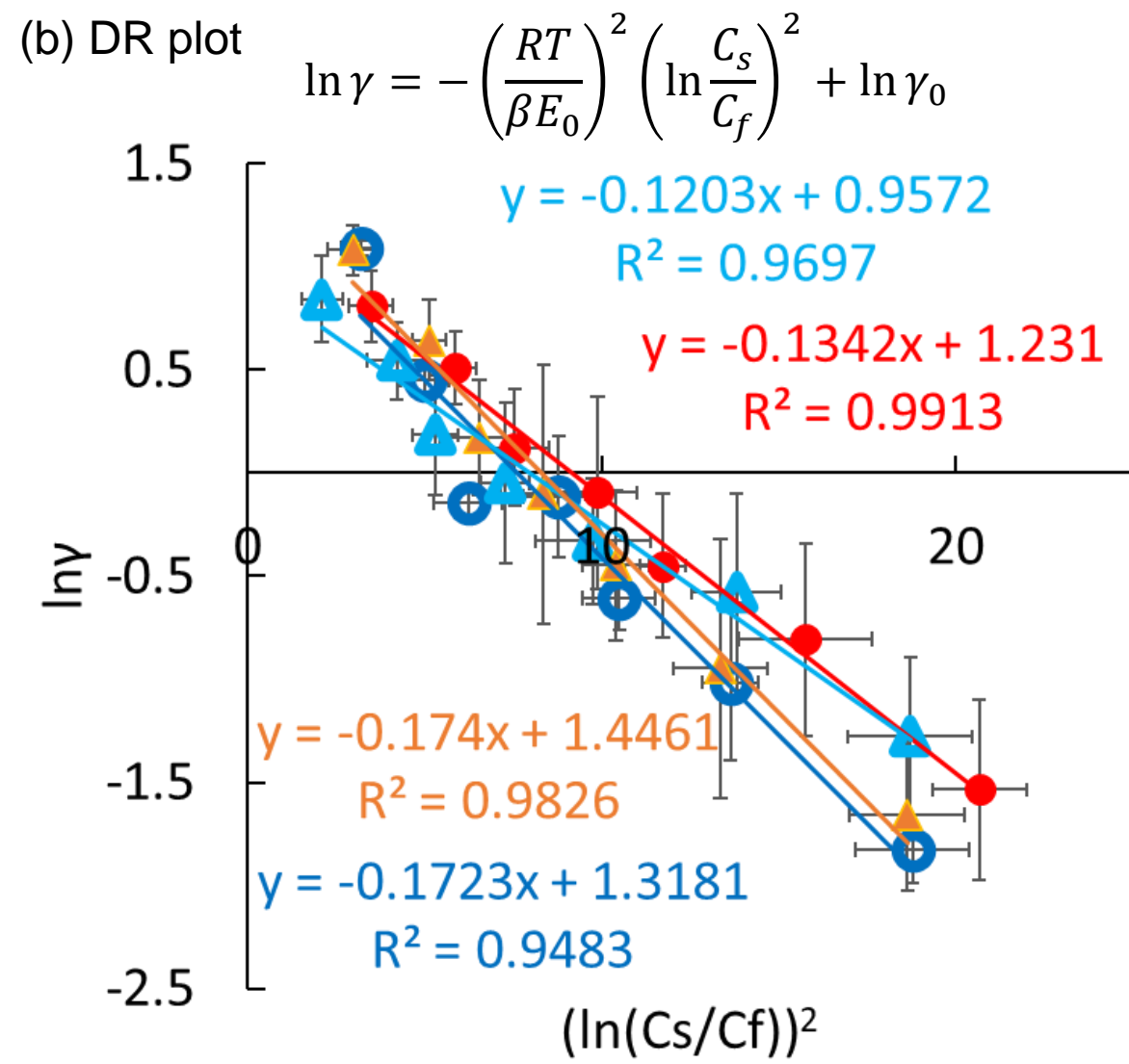
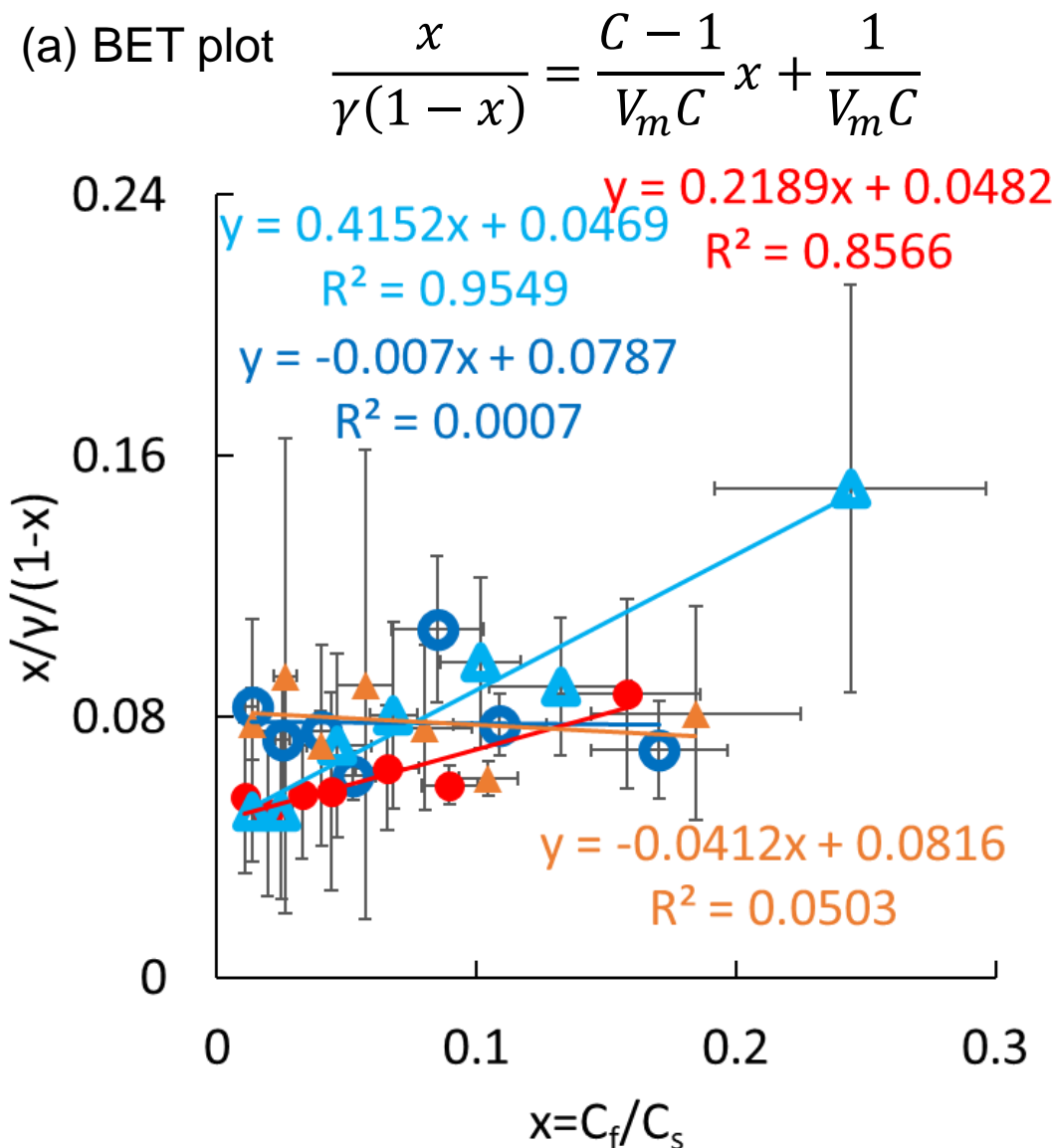


Figure S6. Analyses of heat-treated INS adsorptions on the FCP membranes: hydrophilic (blue open circles) and hydrophobic PVDF (red closed circles), and hydrophilic (light blue open triangles) and hydrophobic PTFE (amber closed triangles), according to BET (a) and DR plots (b). Error bars on the ordinate and abscissa represent standard deviations from three or more experiments.

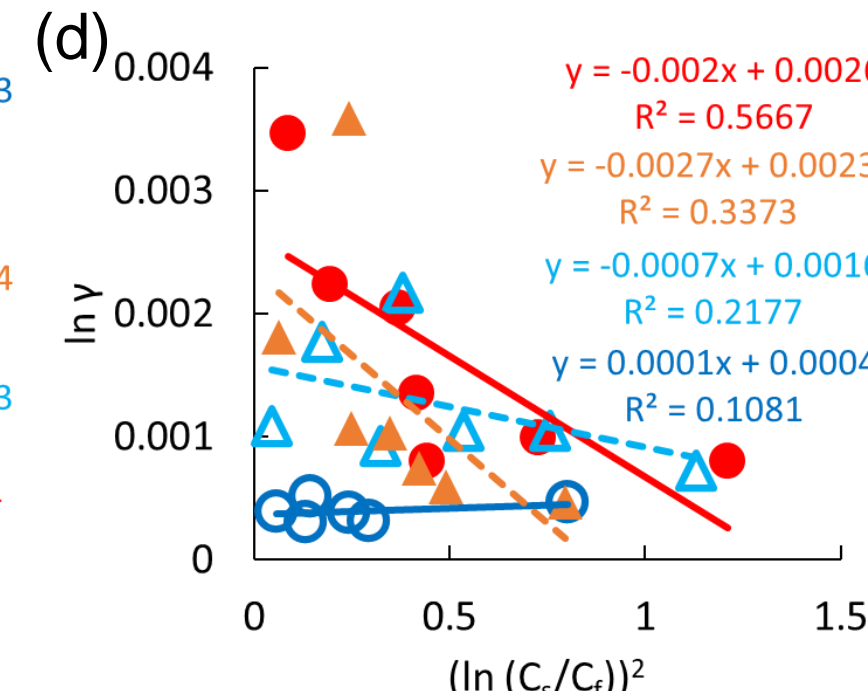
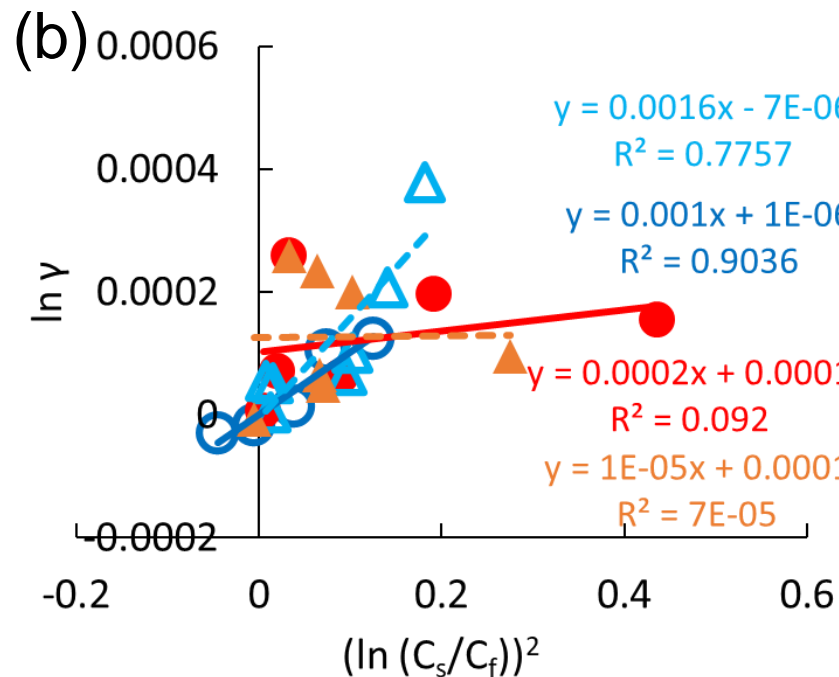
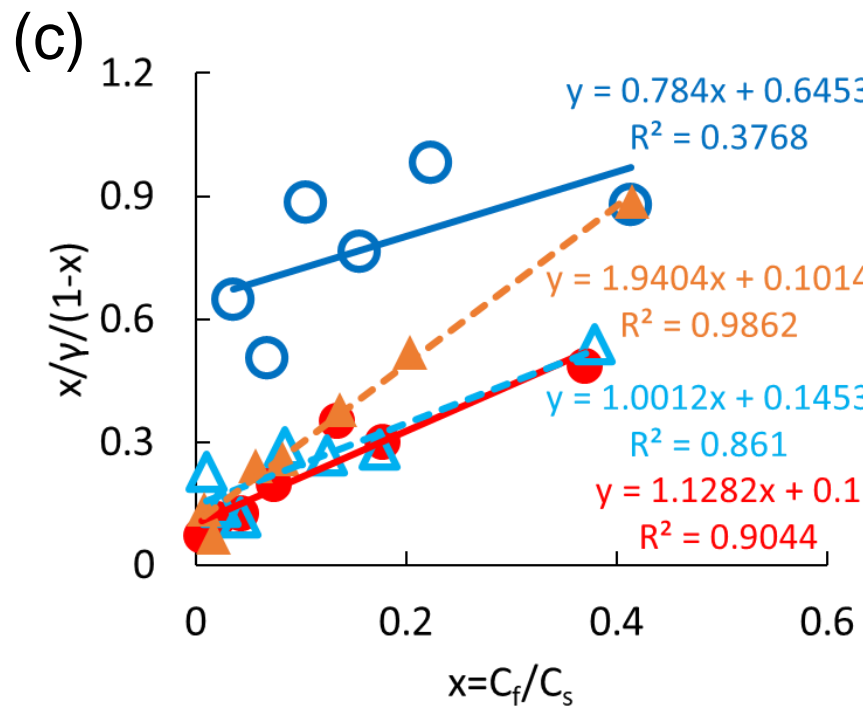
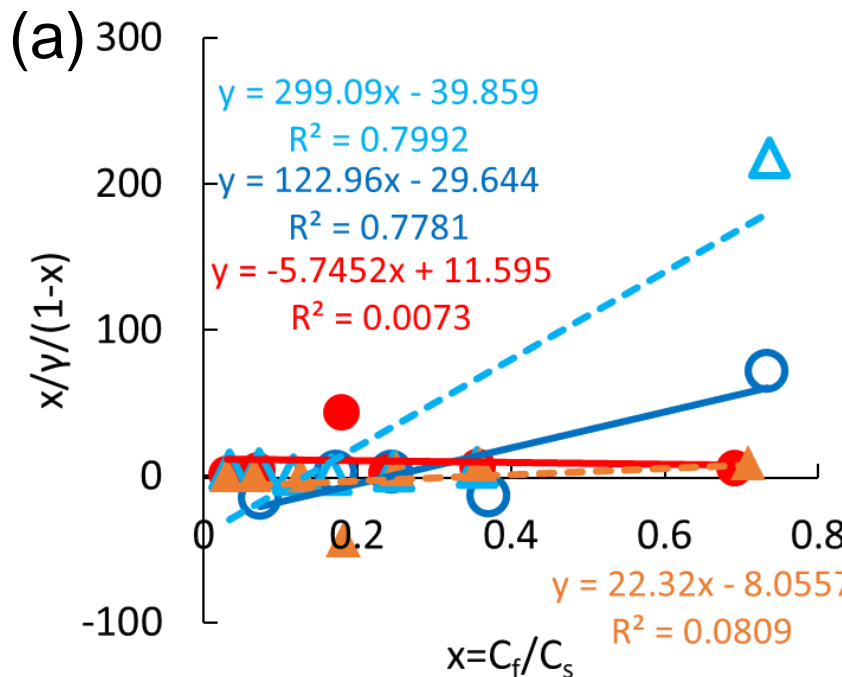


Figure S7. Analyses of BSA (a and b) and ConA (c and d) adsorptions on the FCP membranes: hydrophilic (blue open circles) and hydrophobic PVDF (red closed circles), and hydrophilic (light blue open triangles) and hydrophobic PTFE (amber closed triangles), based on BET (a and c) and DR plots (b and d).

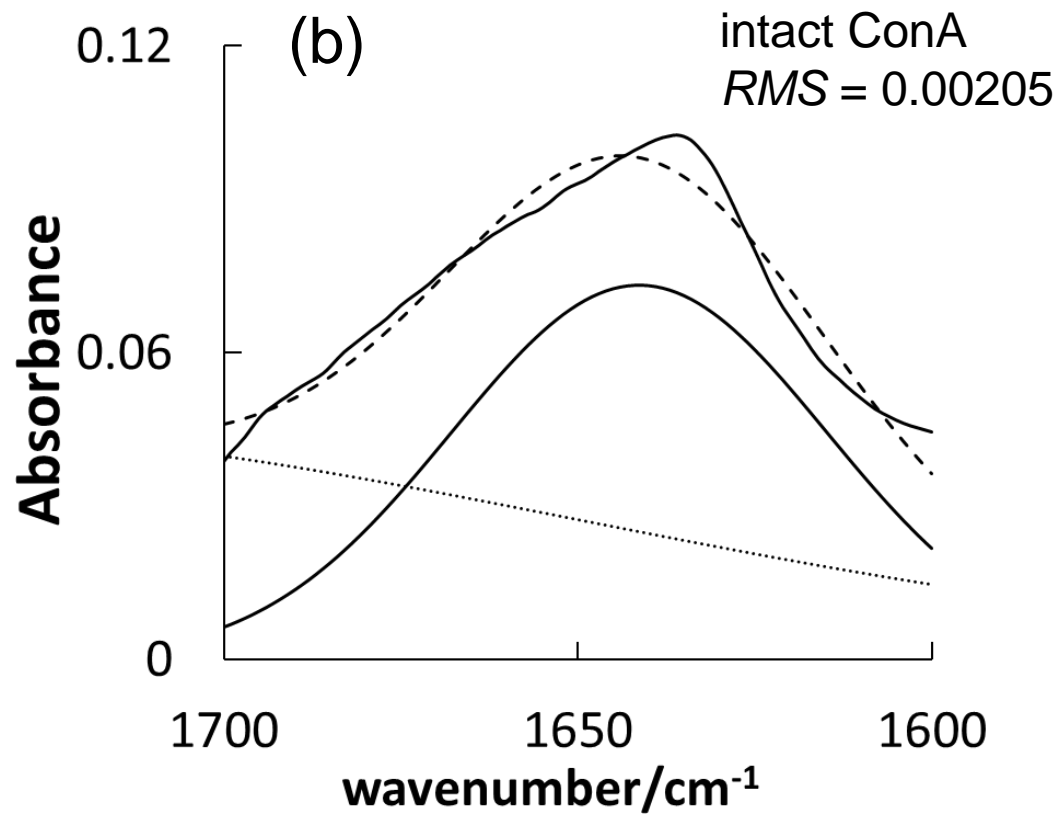
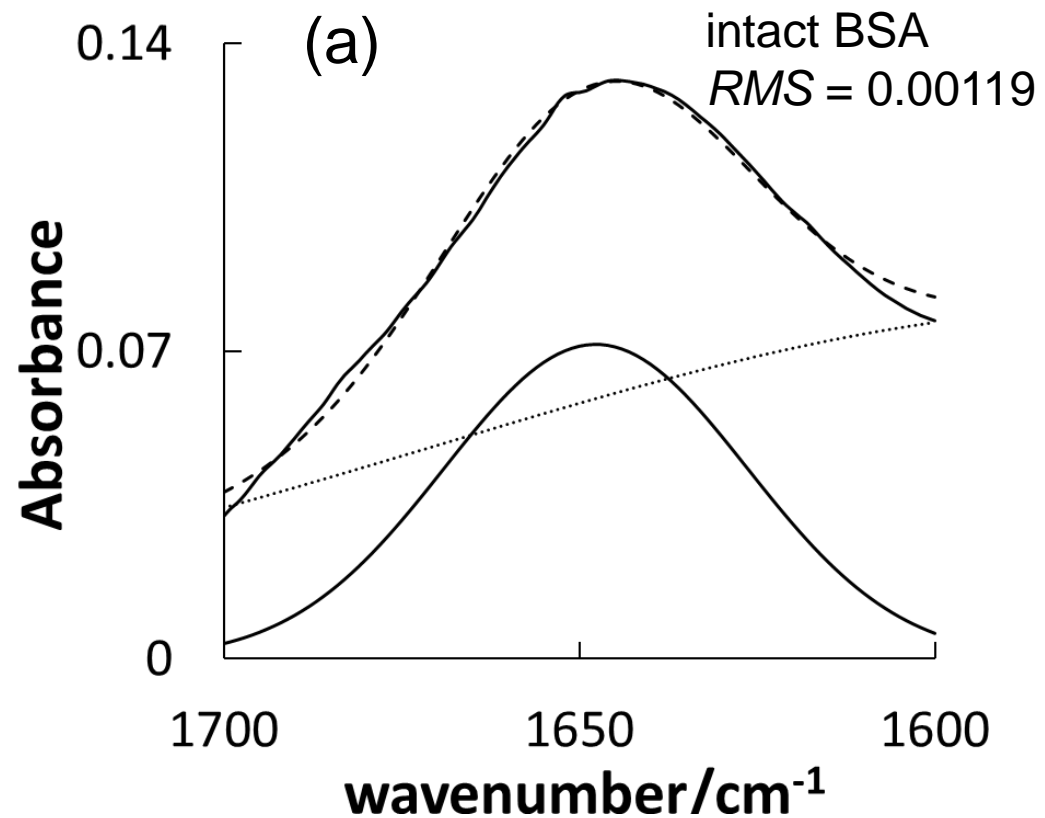


Figure S8. ATR-FTIR spectra of intact BSA (a) and ConA (b) powder at 1700-1600 cm^{-1} wavenumbers. Dashed curves express the curve fitting with Gaussian functions as the components of peaks and baselines. Root-mean-square (RMS) values evaluate the reproductions. As BSA is an α -helix-enriched model, the 1656-1652 cm^{-1} peak was observed in the amide I region. As CoA is the β -sheet-enriched model, the 1622-1637 cm^{-1} peak was observed.

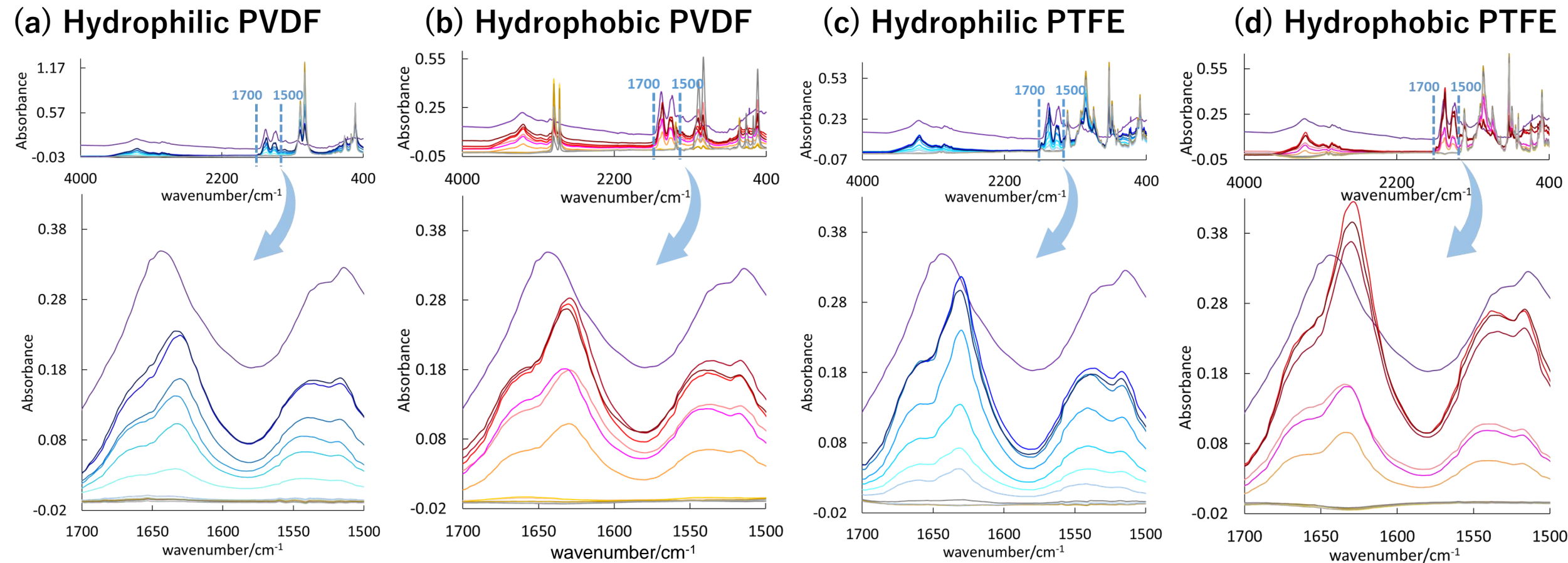
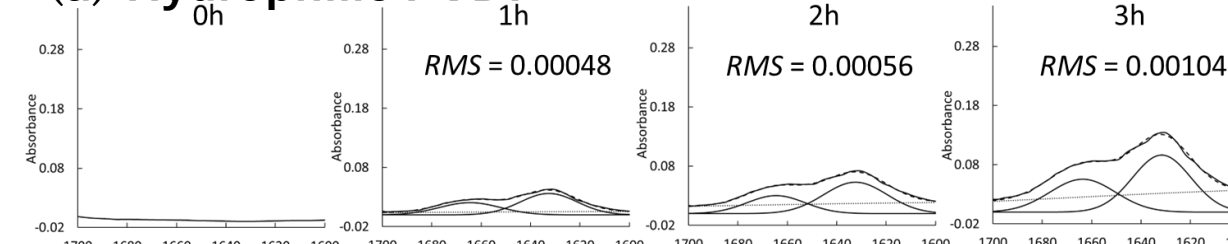
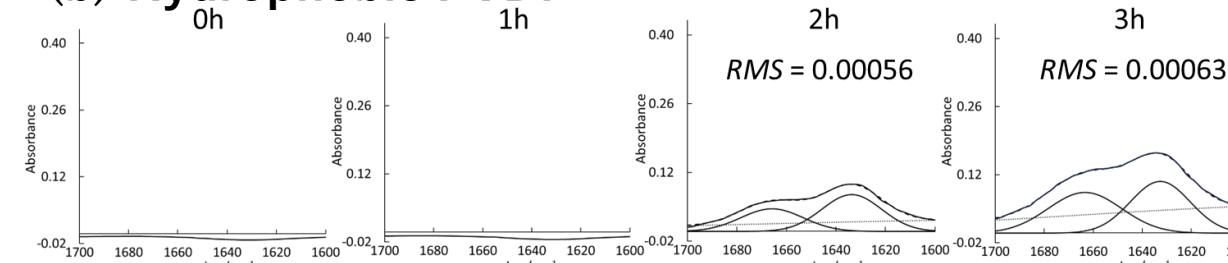


Figure S9. ATR-FTIR spectral changes of heat-treated INS adsorbed on FCP membranes: hydrophilic PVDF (a), hydrophobic PVDF (b), hydrophilic PTFE (c), and hydrophobic PTFE (d). The amide-I bands occur at $1600\text{-}1700\text{ cm}^{-1}$, with α -helix signals at $1648\text{-}1660\text{ cm}^{-1}$ and parallel β -sheet signals at $1610\text{-}1640\text{ cm}^{-1}$. Gray spectra represent the reference sample prepared as the heat-treated INS powder.

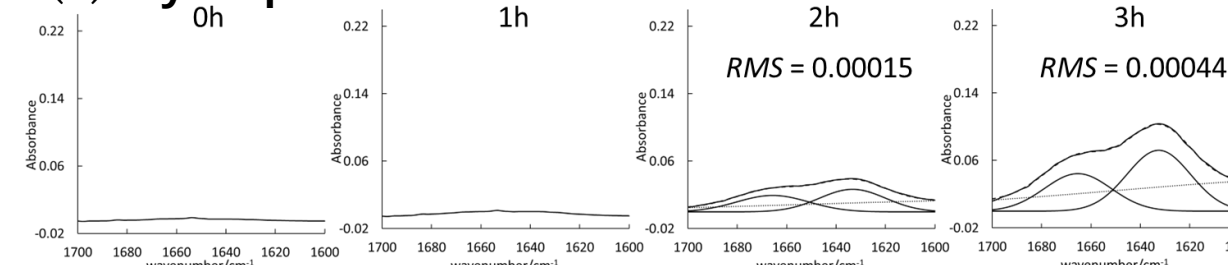
(a) Hydrophilic PVDF



(b) Hydrophobic PVDF



(c) Hydrophilic PTFE



(d) Hydrophobic PTFE

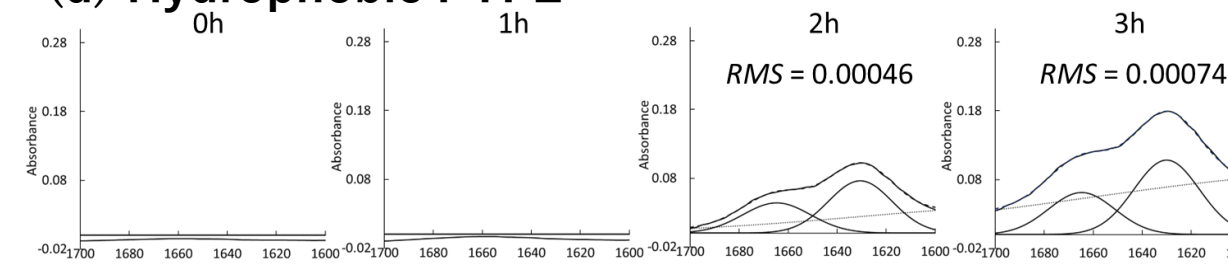
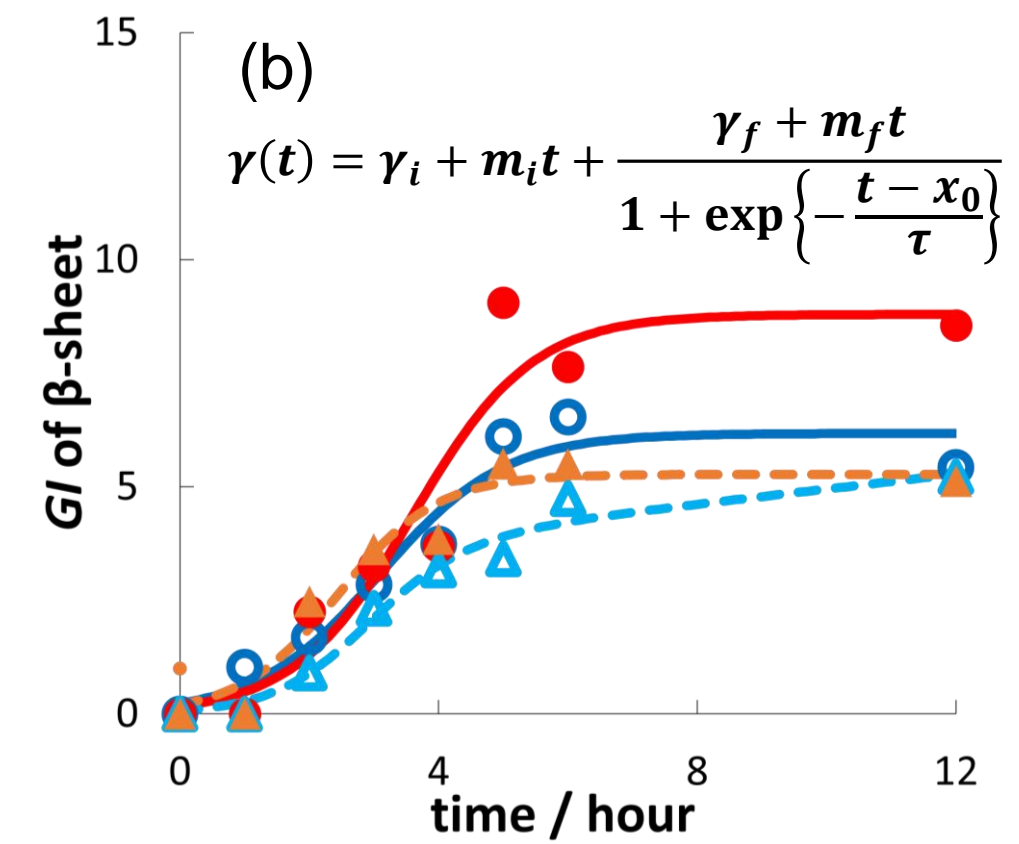
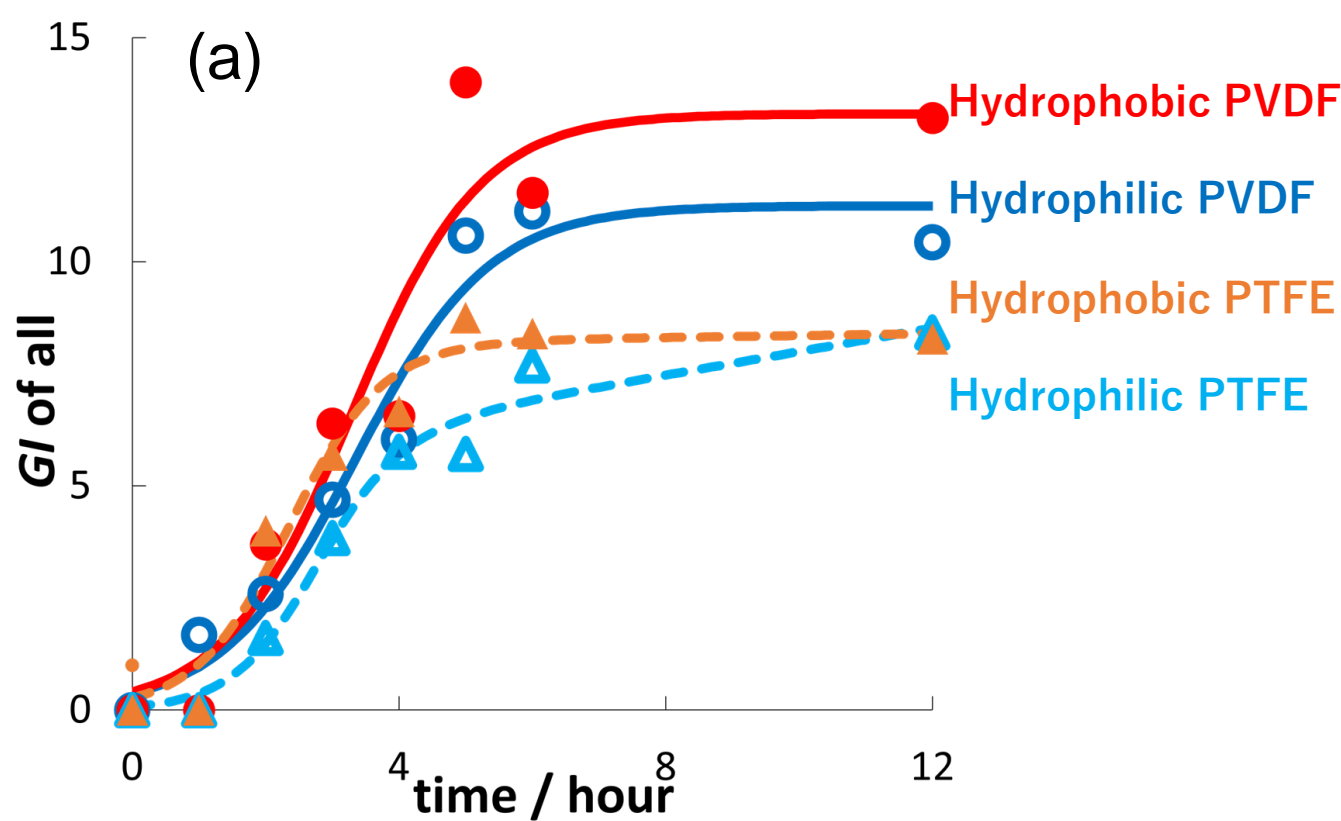


Figure S10. Gaussian fitting of the observed ATR-FTIR spectra of heat-treated INS adsorption (cf. Figure S9)



	hydrophilic PVDF	hydrophobic PVDF	hydrophilic PTFE	hydrophobic PTFE
SS	4.890	16.721	1.418	3.260
m_i	0.000	0.000	0.000	0.000
m_f	0.000	0.000	0.263	0.021
y_f	11.248	13.298	5.371	8.143
x_0	3.358	3.302	2.696	2.349
τ	0.997	0.955	0.637	0.696
lag time (h)	1.364	1.393	1.421	0.957

	hydrophilic PVDF	hydrophobic PVDF	hydrophilic PTFE	hydrophobic PTFE
SS	2.184	7.658	0.651	1.795
m_i	0.000	0.000	0.000	0.000
m_f	0.000	0.000	0.166	0.000
y_f	6.176	8.796	3.293	5.274
x_0	3.095	3.609	2.829	2.449
τ	0.958	0.922	0.751	0.767
lag time (h)	1.180	1.765	1.327	0.914

Figure S11. Curve fitting for time courses of total GI (a) and β -sheet GI values due to the sigmoid function.[26]

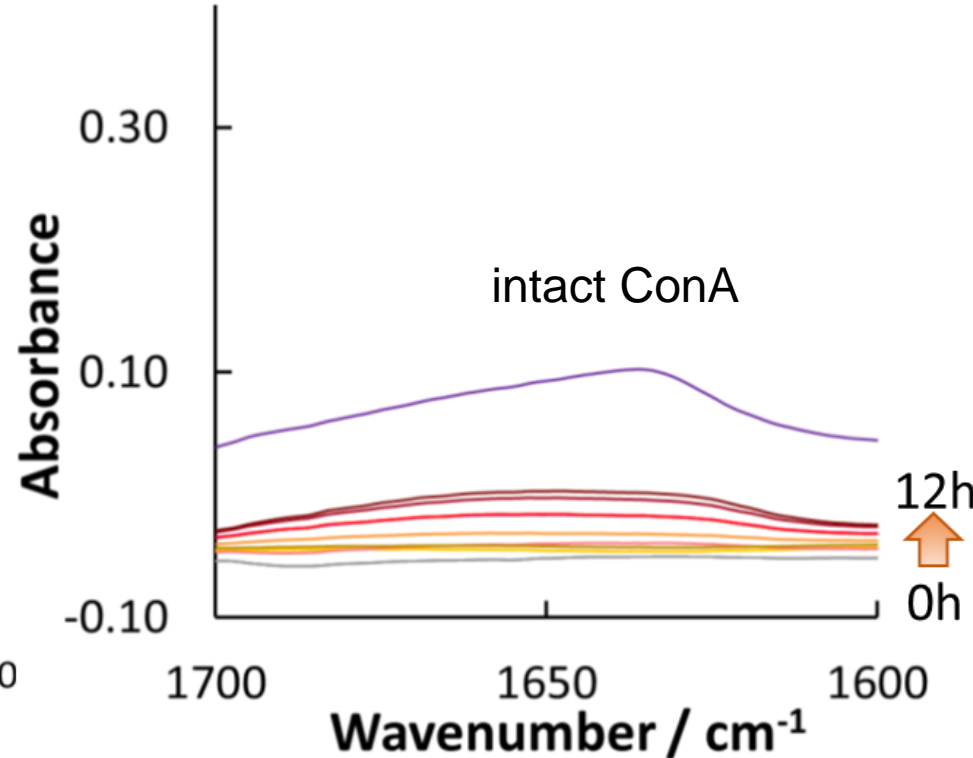
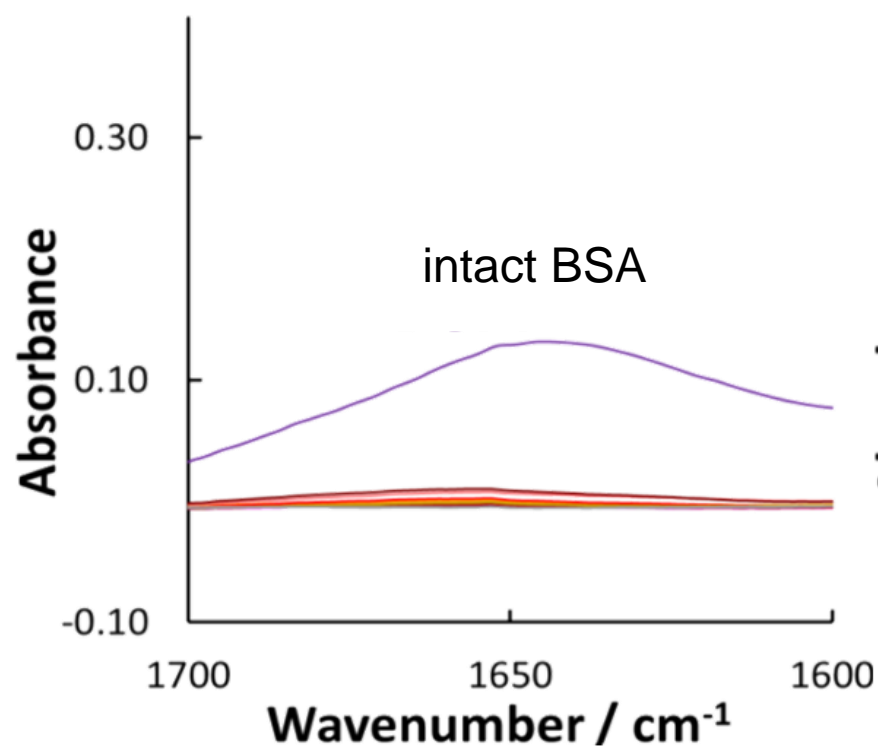


Figure S12. ATR-FTIR spectra of BSA (a) and ConA (b) adsorbed on hydrophobic PVDF at incubation times of 0-12 hours. The spectra of the intact proteins were identical to those in Figure S8.